result in slightly lower estimates for δt. Various experimental probes of W in Rb_3C_{60} with $T_c \approx 30$ K yield estimates in the range 0.1 to 0.5 eV (*15*). For these parameters, we find $|\delta T_c|$ in the range 0.6 to 0.2 K. We reiterate that the absolute magnitude of δt, and hence of δT_c, is difficult to compute to better than a factor of 2 accuracy; the trends, however, as a function of W and T_c implied by Eq. 3 should be reliable and testable experimentally.

REFERENCES AND NOTES

1. B. Serin, C. A. Reynolds, L. B. Nesbitt, *Phys. Rev.* **90**, 761 (1950).
2. S. Chakravarty and S. Kivelson, *Europhys. Lett.* **16**, 751 (1991).
3. S. Chakravarty, M. Gelfand, S. Kivelson, *Science* **254**, 970 (1991).
4. A related effect was studied by D. S. Fisher *et al.* [*Phys. Rev. Lett.* **61**, 482 (1988)] in the context of superconductivity in the cuprates. They studied the effect on T_c of an isotope-dependent shift in an electronic hopping matrix element t, and also made the point that this can lead to an isotope-dependent shift in T_c, even if the mechanism of superconductivity is purely electronic. However, beyond that similarity, there are large differences in the effects we each studied. We studied, which is a specifically molecular feature of the fullerene problem, the influence of the isotope-dependent shift of an intramolecular t on the pair-binding energy. In contrast to the case studied by Fisher *et al.*, the intramolecular t is not expected to be strongly pressure-dependent, so this effect is totally unrelated to the pressure dependence of T_c.
5. T. W. Ebbesen *et al.*, *Nature* **355**, 620 (1992).
6. A. Ramirez *et al.*, *Phys. Rev. Lett.* **68**, 1058 (1992).
7. V. Elser and R. C. Haddon, *Nature* **325**, 792 (1987).
8. S. White, *et. al.*, *Phys. Rev. B* **45**, 5062 (1992).
9. G. Sparn *et al.*, *Phys. Rev. Lett.* **68**, 1228 (1992).
10. C. Kittel, *Introduction to Solid State Physics* (Wiley, New York, ed. 6, 1986).
11. M. I. Salkola, S. Chakravarty, S. A. Kivelson, in preparation.
12. B. T. Kelley and R. Taylor, in *Chemistry and Physics of Carbon*, P. L. Walker and P. A. Thrower, Eds. (Dekker, New York, 1973), vol. 10.
13. In (*12*), the in-plane thermal expansion of graphite was found to be $\kappa = 2 \times 10^{-2}$ Å eV^{-1} at 1400 K. The Debye temperature of graphite is about $\Theta_D \approx 2300$ K, so this is an insufficiently high temperature to measure the asymptotic value. We have obtained an estimate of the asymptotic value of κ by extrapolating the result to high temperatures according to the approximate expression, $\kappa(T) = \kappa_\infty(\Theta_D/2T)^2[\sinh(\Theta_D/2T)]^{-2}$.
14. In L. Salem [*The Molecular Orbital Theory of Conjugated Systems* (Benjamin, Reading, 1974) pp. 134–137], it is noted that the "bond order" is a remarkably linear function of the carbon-carbon bond length. This is suggestive of a linear dependence of t_{ij} on δl_{ij}, that is, $\beta/\alpha \approx 0$. Indeed, as noted by Salem, if the elastic energy due to the σ-electrons is assumed to be quadratic in the displacements, a linear dependence of t_{ij} on δl_{ij} is a direct consequence of the linear dependence of the bond order. On the other hand, if we compute the magnitude of the linear dependence of the bond order on lattice constant using the model of (*11*) with the empirically determined values of the various parameters such as α, we find that the magnitude of the calculated variation of the bond order with bond length is slightly smaller than the observed variation; this discrepancy is consistent with a value of $\beta/\alpha \approx 2$. Of course, there is also some uncertainty in the values of α and the σ-bond spring constant, K, and the inferred value of β is very sensitive to small changes in these other parameters. If t_{ij} were a pure exponential function of l_{ij}, this would imply $\beta/\alpha \approx 3$.
15. L. D. Rotter *et al.*, *Nature* **355**, 532 (1992).

16. This work was supported in part by the National Science Foundation (grants DMR-89-07664 and DMR-90-11803) and in part by the Office of Naval Research (N00014-92-J-1101).

3 April 1992; accepted 29 April 1992

Presence of the Earliest Vertebrate Hard Tissues in Conodonts

I. J. Sansom, M. P. Smith, H. A. Armstrong, M. M. Smith

From histological investigations into the microstructure of conodont elements, a number of tissue types characteristic of the phosphatic skeleton of vertebrates have been identified. These include cellular bone, two forms of hypermineralized enamel homologs, and globular calcified cartilage. The presence of cellular bone in conodont elements provides unequivocal evidence for their vertebrate affinities. Furthermore, the identification of vertebrate hard tissues in the oral elements of conodonts extends the earliest occurrence of vertebrate hard tissues back by around 40 million years, from the Middle Ordovician (475 million years ago) to the Late Cambrian (515 million years ago).

Since their first description (*1*), debate over the phylogenetic affinities of conodonts has persisted, encompassing such diverse groups as algae, vascular plants, numerous invertebrate phyla, chordates, and vertebrates (*2*). The recent discovery and interpretation of conodonts with preserved soft tissue (*3, 4*) has led to increased support for chordate affinity (*4, 5*), although alternative hypotheses based on the soft-bodied specimens have postulated a relation with aplacophoran mollusks (*6*) or chaetognaths (*7*). The group has also been considered to possess sufficient novel characters to warrant phylum status (*8*).

The only hard parts of these animals, the conodont elements, are composed of carbonate fluorapatite (*9*) with a matrix of collagen and other organic material (*10*). Elements are located in the oral cavity and are thought to have had a food-processing function analogous with teeth (*11*). They are internally divisible into a basal body, lamellar crown, and white matter (*12*) (Figs. 1A, 2A, and 3, A and D). Given the chemical and morphological similarity of the elements to vertebrate tissues, it has been variously proposed that the lamellar crown is homologous with enamel (*13*), enameloid (*5, 14*), acellular bone (aspidin) (*15*), or the unmineralized keratinous teeth of myxinoids (*16*), whereas the basal tissue has been compared with dentine (*5, 13, 14*), bone (*18*), and cartilage (*18*). Previous studies have not, however, clearly demonstrated histological homology between conodont elements and vertebrate teeth (*19*), and it has generally been concluded that the elements are composed of tissue types confined to conodonts. White matter, in particular, has been regarded as a novel and enigmatic tissue, arising from secondary modification of the lamellar crown (*20*), although Krejsa *et al.* (*16*) proposed homology between white matter microspaces and tubules in *Ozarkodina confluens* (Branson and Mehl) and structures associated with pokal cells and parakeratotic keratin in the lingual elements of myxinoids.

The conodont elements we have prepared (*21*) were compared with similar preparations of vertebrate skeletal material from the Harding Sandstone, Canon City, Colorado, the earliest unequivocal vertebrate hard tissues that are histologically intact (*22, 23*). Three genera are present in the Harding material (*14, 19*), each with a distinct histological association. Sclerites of *Astraspis* Walcott and *Eriptychius* Walcott are both composed of basal acellular bone (aspidin) and superficial tubercles of acellular dentine, capped by enameloid and enamel, respectively. A third, unnamed, genus has discrete tubercles composed of cellular bone and cellular dentine, and may represent a stem group osteostracan (*22*).

White matter is consistently developed in all of the conodont specimens examined to date. It is characterized by lacunate spaces, interconnected by irregular, radiating tubules (Figs. 1D, 2C, and 3, B

I. J. Sansom and H. A. Armstrong, Department of Geological Sciences, University of Durham, South Road, Durham DH1 3LE, United Kingdom.
M. P. Smith, School of Earth Sciences, University of Birmingham, Edgbaston, Birmingham B15 2TT, United Kingdom.
M. M. Smith, Division of Anatomy and Cell Biology, United Medical and Dental Schools of Guy's and St. Thomas's Hospitals, London Bridge, London SE1 9RT, United Kingdom.

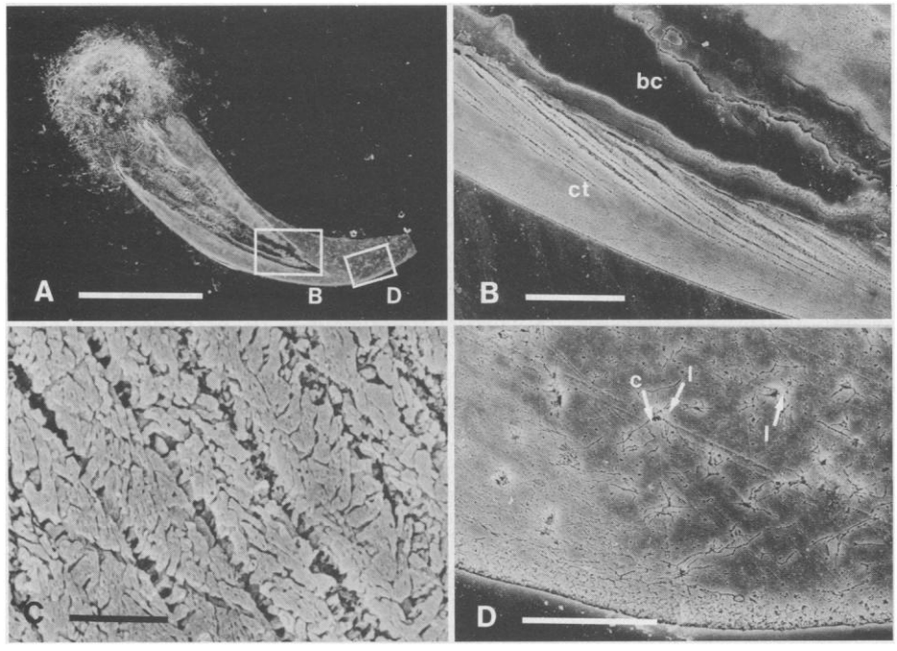

Fig. 1. Scanning electron micrographs of an element of the panderodontid conodont *Panderodus unicostatus* (Branson and Mehl) (BU 2155) from the Ludlow of the tramway section, Netherton, West Midlands, United Kingdom. (**A**) Element in longitudinal section showing the relation between lamellar tissue, white matter, and basal cavity; there is no basal body occupying the basal cavity in this specimen. The material that apparently occupies the upper half of the basal cavity is part of the lamellar crown; the difference in appearance is a sectioning artifact. Scale bar, 200 μm. (**B**) One of the boxed areas in (A) showing part of the basal cavity (bc) and lamellar crown tissue (ct). The lamellae are asymptotic to the external surface, indicating that the growth of *Panderodus* elements in later stages was dominated by basal extension and widening. Scale bar, 20 μm. (**C**) Subparallel orientation of apatite crystallites within the lamellar tissue, typical of *Panderodus* and closely related genera. The porous interlamellar zones are thought to represent poorly mineralized, organic-rich zones produced during interruptions in growth. Scale bar, 2 μm. (**D**) Detail of white matter boxed in (A) showing well-developed lacunae (l) and interconnecting, radiating canaliculi (c). The interconnecting nature of the canaliculi has been confirmed by confocal microscopy and Nomarski interference optics. The presence of cell spaces, interconnecting canaliculi, and the massive ground mass are indicative of cellular dermal bone. Scale bar, 20 μm. Each micrograph was taken at 15 kV.

and E) which, together with the relatively lower level of biological mineralization, give the tissue its characteristic opaque appearance in incident light. These spaces are identical with those of osteocyte lacunae and canaliculi of both fossil and recent cellular bone (the spaces for cell bodies and their extending processes, respectively), and we consider them to be homologous. The lacunae in the white matter are from 3 to 10 μm in diameter, a range that overlaps with those of osteocytes in the cellular bone of the unnamed Harding Sandstone genus (*22*). Previous hypotheses stating that white matter is a secondary replacement of the lamellar crown tissue (*20*) appear to be untenable since there are no relicts of either the lamellar structure or the characteristic arrangement of crystallites. Specimens of *Ozarkodina* also show similar canaliculi (Fig. 3B) and the interpretation of the spaces as pokal cell processes (*16*) is not tenable.

The lamellar part of the conodont element crown shows incremental lines in a centrifugally deposited tissue, with each lamella bounded by nonmineralized areas that probably represent interruptions of growth. Two types of lamellar crown tissue can be recognized. In elements of *Cordylodus* Pander and *Ozarkodina*, the crystallites are oriented perpendicular to the lamellae (Figs. 2, A and B, and 3C). The perpendicular arrangement of crystallites and the presence of incremental lines are typical of hypermineralized ectodermally derived tissues such as enamel

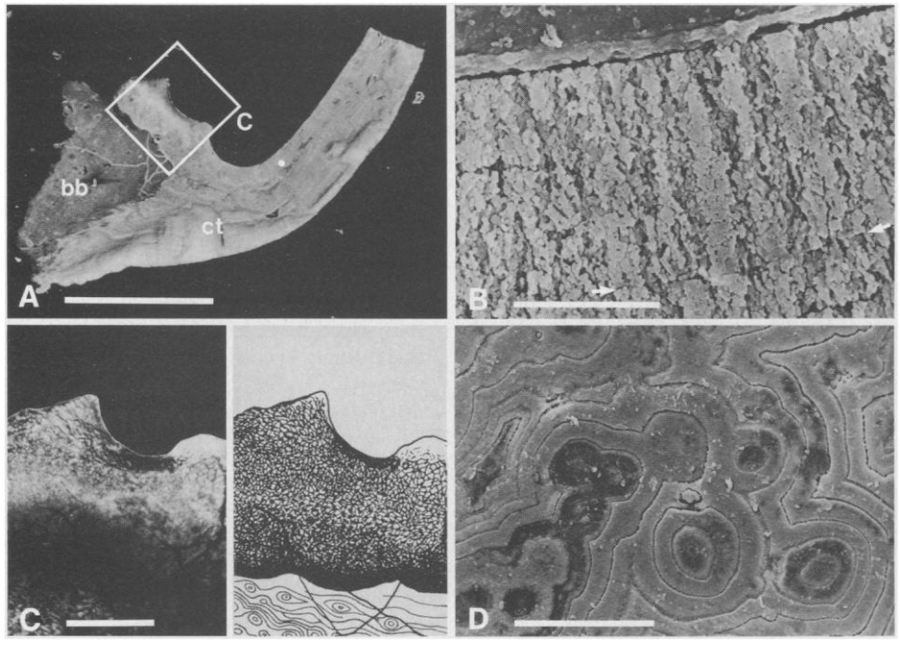

Fig. 2. Longitudinal section of an element of *Cordylodus* Pander (BU 2156) from the Tremadoc of Maardu, Estonia. (**A**) Scanning secondary electron micrograph of the specimen following acid etching, showing the differentiation into crown tissue (ct) and basal body (bb) together with increment lines within the crown. Scale bar, 200 μm. (**B**) At higher magnification, crystallites of the crown are seen to be organized into prisms oriented transversely to the growth lamellae (arrows). Note the contrast in crystallite orientation between *Cordylodus* and *Panderodus* (Fig. 1C). The former has a structure closely similar to enamel, but the latter is enigmatic and may represent a new form of hypermineralized epidermally derived tissue. Scale bar, 5 μm. (**C**) Micrograph and drawing of the two denticles boxed in (A), viewed under partial Nomarski optics. Although white matter is present throughout the element cusp, the greatest concentration is found in the denticle cores, where cell lacunae and interconnecting canaliculi are clearly seen throughout (see drawing). Scale bar, 75 μm. (**D**) Scanning electron micrograph (SEM) of the basal body showing the spherulitic appearance of this tissue. The internal structure of the basal body is directly comparable with globular calcified cartilage found in *Eriptychius* from the Harding Sandstone and other vertebrates. Scale bar, 20 μm. SEMs taken at 15 kV.

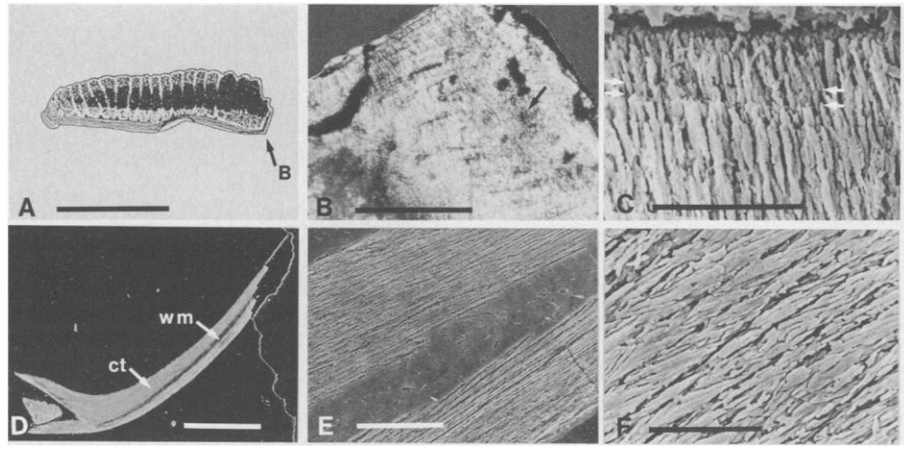

Fig. 3. (**A**) Line drawing of an oblique section through a Pa element of *Ozarkodina confluens* (Branson and Mehl) (BU 2157) from the Llandovery of Själsö, Gotland, Sweden, showing the distribution of tissues. Cellular white matter forms the denticle cores surrounded by lamellar crown tissue. Scale bar, 200 μm. (**B**) Detail of the part of the element arrowed in (A), taken in Nomarski interference contrast. The superimposition of the lamellar crystallite pattern onto the core of cellular white matter (black arrow) is a cut artifact. Scale bar, 50 μm. (**C**) Scanning secondary electron micrograph of the lamellar crown tissue showing the orientation of the apatite crystallites perpendicular to the growth surface, and hence cutting across the increment lines (arrows). Scale bar, 5 μm. (**D**) Scanning secondary electron micrograph of an element of the panderodontid conodont *Parapanderodus striatus* (Graves & Ellison) (MGUH 21142, sample GGU 274944) from the late Canadian (Early Ordovician) of Kronprins Christian Land, North Greenland, illustrating the distribution of the lamellar crown tissue (ct) and the central core of white matter (wm). Scale bar, 200 μm. (**E**) Electron micrograph detailing the relationship between the lamellar crown and the cellular white matter. The white matter shows a cone-in-cone structure and a sharp contact with the surrounding tissue. Scale bar, 20 μm. (**F**) Detail of the lamellar crown tissue showing the subparallel orientation of the crystallites with respect to the lamellae, this tissue is typical of panderodontid lamellar crown (compare Fig. 1C). Scale bar, 5 μm.

(*24*). A second type of lamellar tissue is present in elements of *Panderodus* (Branson and Mehl) and *Parapanderodus* Stouge and is characterized by crystallites oriented with their long axes subparallel to the growth surface (Figs. 1, B and C, and 3, E and F). This tissue is enigmatic, but may represent a new type of hypermineralized hard tissue related to enamel and identified to date only in panderodontid conodonts.

All specimens with intact basal bodies show a clear structure in which discrete spherules are fused into continuous scalloped layers (Fig. 2D) with the boundaries formed as Liesegang waves (*25*). Basal bodies with a similar spherulitic structure have been illustrated in a number of conodont taxa from North America (*20*), Siberia (*17*), and Europe (*7*). Although it is possible that other mineralization processes could produce spherulitic structures such as these, they bear a striking resemblance to the globular calcified cartilage found in *Eriptychius* and certain other vertebrates (*19*).

The recognition of cellular bone in conodonts has important implications for studies of both conodont palaeobiology and early vertebrate evolution:

1) Cellular bone is a hard tissue unique to vertebrates, and its occurrence in conodont elements is unequivocal evidence for the inclusion of conodonts within the vertebrates. The additional presence of enamel homologs and probable globular cartilage is consistent with this conclusion.

2) The presence of cellular bone in the Late Cambrian–earliest Ordovician genus *Cordylodus* predates the earliest previously recorded occurrence of vertebrate hard tissues by around 40 million years.

3) Although the tissues within conodont elements have been identified and homologized with those in vertebrates, their growth sequence remains unelucidated. The presence of cellular bone and of lamellae tangential to the element margin means that the widely accepted growth mechanism of Bengtson (*26*) is, at best, oversimplified and must be reassessed.

4) It is frequently assumed that early vertebrate hard tissues evolved as a generalized dermal armor composed of small individual denticles and that they became increasingly specialized in a feeding function with time (*27*). In contrast, the discovery of the earliest vertebrate hard tissues in the oral feeding apparatus of conodonts indicates that the first hard tissues were highly specialized, with a function not dissimilar to that adopted by later vertebrates.

5) Dentine has been proposed as one of the primitive vertebrate hard tissues (*20*). The conodont elements examined contain cellular bone, enamel-like tissues, and cartilage but no dentine, casting doubt on the assumed evolutionary primacy and functional origin of dentine.

6) The most widely cited phylogenetic classification of lower vertebrates (*4, 19, 28, 29*) recognizes cellular dermal bone as an advanced craniate synapomorphy linking the osteostracans and gnathostomes. The presence of cellular bone and the absence of dentine in Cambrian conodonts indicates that the evolutionary history of vertebrate hard tissues must be reevaluated.

REFERENCES AND NOTES

1. C. H. Pander, *Akad. Wiss., St. Petersburg* **10**, 1 (1856).
2. K. J. Müller, in *Treatise on Invertebrate Paleontology, Part W, Supplement 2, Conodonta*, R. A. Robinson, Ed. (Geological Society of America and Univ. of Kansas Press, Lawrence, KS, 1981), pp. W78–W82.
3. D. E. G. Briggs *et al.*, *Lethaia* **16**, 1 (1983).
4. R. J. Aldridge *et al.*, *ibid.* **19**, 279 (1986).
5. J. Dzik, in *Problematic Fossil Taxa*, A. Hoffman and M. H. Nitecki, Eds. (Oxford Univ. Press, New York, 1986), pp. 240–254.
6. S. Tillier and J.-P. Cuif, *C. R. Acad. Sci. Paris* **303 Ser. II**, 627 (1986); S. Tillier and P. Janvier, *Recherche* **17**, 1574 (1986). This hypothesis of aplacophoran affinity was subsequently refuted by D. E. G. Briggs, R. J. Aldridge, and M. P. Smith [*Lethaia* **20**, 381 (1987)].
7. H. Szaniawski, in *Palaeobiology of Conodonts*, R. J. Aldridge, Ed. (Ellis Horwood, Chichester, U.K., 1987), pp. 35–47.
8. W. C. Sweet, *The Conodonta: Morphology, Taxonomy, Paleoecology, and Evolutionary History of a Long-Extinct Animal Phylum* (Oxford Univ. Press, New York, 1988).
9. H. Pietzner, J. Vahl, H. Werner, W. Ziegler, *Palaeontographica Abt A* **128**, 115 (1968).
10. L. E. Fåhræus and G. E. Fåhræus-van Ree, in *Palaeobiology of Conodonts*, R. J. Aldridge, Ed. (Ellis Horwood, Chichester, 1987), pp. 105–110.
11. L. Jeppsson, *Lethaia* **12**, 153 (1979); R. J. Aldridge, M. P. Smith, R. D. Norby, D. E. G. Briggs, in *Palaeobiology of Conodonts*, R. J. Aldridge, Ed. (Ellis Horwood, Chichester, 1987), pp. 63–75.
12. M. Lindström, *Conodonts*, (Elsevier, Amsterdam, 1964).
13. H. Schmidt and K. J. Müller, *Paläont. Z.* **38**, 105 (1964); D. Andres, *Palaeontographica Abt A* **200**, 105 (1988).
14. R. H. Denison, *Clin. Orthop.* **31**, 141 (1963).
15. W. Gross, *Senckenberg. Leth.* **35**, 73 (1954).
16. R. J. Krejsa, P. Bringas, Jr., H. C. Slavkin, *Lethaia* **23**, 359 (1990).
17. I. S. Barskov, T. A. Moskalenko, L. P. Starostina, *Paleont. Zh.* **1982(2)**, 82 (1982).
18. G. A. Stewart and W. C. Sweet, *J. Paleont.* **30**, 261 (1956).
19. M. M. Smith and B. K. Hall, *Biol. Rev.* **65**, 277 (1990).
20. C. R. Barnes, D. B. Sass, M. L. S. Poplawski, *Life Sci. Contr. R. Ont. Mus.* **90**, 1 (1973).

21. Double polished specimens, 60 to 80 μm thick, were examined using polarized light, phase contrast, Nomarski interference contrast, and SEM. For the latter, specimens were polished with 0.05-μm alumina powder, and subsequently etched in a 0.5% (by weight) solution of $CrSO_4$ buffered to a pH of 3.5 using NaOH following the methodology of B. Sundström [*Odont. Revy* **19** (*Suppl. 13*), 1 (1968)]. A total of 23 species representing 16 genera and 10 conodont families have been examined to date and range in age from Late Cambrian to Silurian. All have white matter that contains cell lacunae and canaliculi similar to those in the specimens figured.
22. M. M. Smith, *Science* **251**, 301 (1991).
23. Although older (late Arenig or early Llanvirn) vertebrate material has been described from Australia by A. Ritchie and J. Gilbert-Tomlinson [*Alcheringa* **1**, 351 (1977)], no original hard tissues are preserved and their histology is consequently unknown. Vertebrates are here considered synonymous with craniates, following the definition of R. P. S. Jefferies [*The Ancestry of Vertebrates* (British Museum, Natural History, London, 1988)].
24. M. M. Smith, *Hist. Biol.* **3**, 97 (1989).
25. T. Ørvig, *Zool. Scr.* **18**, 427 (1989).
26. S. Bengtson, *Lethaia* **9**, 185 (1976).
27. T. Ørvig, in *Current Problems in Lower Vertebrate Phylogeny*, T. Ørvig, Ed. (Almquist & Wiksell, Stockholm, 1968) pp. 374–397; W.-E. Reif, *Evol. Biol.* **15**, 287 (1982).
28. P. Janvier, *J. Vert. Paleontol.* **1**, 121 (1981).
29. L. B. Halstead, in *Problems of Phylogenetic Reconstruction*, K. A. Joysey and A. E. Friday, Eds. (Academic Press, London, 1982), pp. 159–196.
30. We would like to express our thanks to G. R. Coope and R. J. Aldridge for their valuable comments on variants of the manuscript, and to the latter for also supplying Estonian conodont material. T. Whitfield and G. A. Parker provided technical assistance and the use of facilities at the University of Newcastle upon Tyne and the University of Durham is acknowledged. The illustrated specimens prefixed BU are deposited in the Lapworth Museum, School of Earth Sciences, University of Birmingham, and that with the prefix MGUH is held at the Geological Museum, Copenhagen, Denmark.

31 January 1992; accepted 9 April 1992

Natural Versus Anthropogenic Factors Affecting Low-Level Cloud Albedo over the North Atlantic

Paul G. Falkowski, Yongseung Kim, Zbigniew Kolber, Cara Wilson, Creighton Wirick, Robert Cess

Cloud albedo plays a key role in regulating Earth's climate. Cloud albedo depends on column-integrated liquid water content and the density of cloud condensation nuclei, which consists primarily of submicrometer-sized aerosol sulfate particles. A comparison of two independent satellite data sets suggests that, although anthropogenic sulfate emissions may enhance cloud albedo immediately adjacent to the east coast of the United States, over the central North Atlantic Ocean the variability in albedo can be largely accounted for by natural marine and atmospheric processes that probably have remained relatively constant since the beginning of the industrial revolution.

The albedo of clouds is an important but poorly understood factor influencing Earth's radiation budget (*1*) that depends nonlinearly on column-integrated liquid water content and the concentration of cloud condensation nuclei (CCN) (*2*). There is evidence that over land cloud albedo increases as cloud temperature increases (*3*). Hence, over the ocean, low-level cloud albedo might be expected to be high where sea surface temperature (SST) is also high. CCN are composed largely of submicrometer-sized aerosol sulfate particles, which have both natural and anthropogenic sources. Over the oceans, phytoplankton production of dimethyl sulfide (DMS), which outgases and is oxidized to form aerosol sulfate, has been suggested to be a major source of CCN (*2*, *4*). In the Northern Hemisphere, however, the emissions of anthropogenic, continentally derived sulfate are approximately five times the emissions from natural marine sources (*5*).

In examining satellite images over the North Atlantic Ocean, we noted that the albedo of marine stratus clouds showed systematic trends over large distances (Figs. 1 and 2). In particular, in a latitude band corresponding to the highest anthropogenic sulfate fluxes from the North American continent, albedo generally decreased from the western to eastern regions of the Atlantic basin (Fig. 2B). This gradient suggests that emissions of anthropogenic continental sulfate may affect the albedo of oceanic clouds thousands of kilometers from the coast. We examined the relative importance of anthropogenic and natural factors on the albedo of marine stratus clouds by comparing the seasonal, basin-scale distributions among upper ocean phytoplankton biomass (using chlorophyll as a proxy), SST, and low-level cloud albedo for the North Atlantic Ocean.

We elucidated the contribution of phytoplankton sources of CCN to the albedo of marine stratus clouds by comparing gridded, monthly averaged, low-level cloud albedos derived from the Earth Radiation Budget Experiment (ERBE) satellite data (*1*) with composited, surface ocean chlorophyll concentrations derived from the Coastal Zone Color Scanner (CZCS). The ERBE data, obtained from the National Oceanic and Atmospheric Administration NOAA-9 scanner measurements, were selected for the North Atlantic Ocean and analyzed for four representative midseason months: April, July, and October 1985 and January 1986. The NOAA-9 satellite is in a sun-synchronous orbit and crosses the equator at 1430 local time. The data were screened so as to include only totally overcast pixels, and a longwave filter (*6*) was then used to isolate warm and thus low-altitude clouds (primarily marine stratus). Because the satellite was in a sun-synchronous orbit, the effect of variations in solar zenith angle on albedo at a fixed latitude was largely eliminated in any given month. Albedos were calculated across seven zonal latitude bands, between 28° and 60°N (Fig. 1, left). Within each band, all pixels (approximately 50 km in diameter at nadir) for a given month were averaged for each 1° of longitude. In all, 28 submaps (corresponding to seven latitude bands and 4 months) of albedo were constructed, from the western edge of the North Atlantic basin to 20°W. At lower latitudes, in warmer months, the paucity of stratus clouds did not permit further analyses.

To obtain representative surface phytoplankton distributions, we used the entire CZCS data set for the North Atlantic Ocean. The sensor, which flew aboard Nimbus-7 between November 1978 and May 1986, acquired global observations of ocean color. Upper ocean chlorophyll concentrations were calculated from water-leaving radiances with atmospheric corrected algorithms (*7*). The spatial coverage of CZCS data for any given month was not sufficient to allow a direct monthly comparison with the albedos calculated from the ERBE data; the temporal overlap between CZCS and ERBE satellites occurred when the CZCS data transmissions were most sparse. However, the interannual variations in chlorophyll within any region

Table 1. The regional distribution of continental sulfur dioxide and sulfate sources for seven latitude bands compiled from the NAPAP data base (*9*) (units are tons per year).

Latitude band	SO_2	SO_4^{2-}	$SO_2 + SO_4^{2-}$
57°–60°N	199,655	56	199,711
52°–57°N	816,286	46,147	862,433
47°–52°N	1,428,974	33,716	1,462,690
43°–47°N	2,899,895	83,822	2,983,717
38°–43°N	12,490,324	223,553	12,713,877
33°–38°N	5,793,258	140,648	5,933,906
28°–33°N	3,118,539	53,781	3,172,320

P. G. Falkowski, Z. Kolber, C. Wilson, C. Wirick, Oceanographic and Atmospheric Sciences Division, Brookhaven National Laboratory, Upton, NY 11973.
Y. Kim and R. Cess, Institute for Terrestrial and Planetary Atmospheres, State University of New York, Stony Brook, NY 11794.